BULLETIN OF THE POLISH ACADEMY OF SCIENCES
TECHNICAL SCIENCES, Vol. 71(5), 2023, Article number: e146238
DOI: 10.24425/bpasts.2023.146238

Application of high-speed camera measurements for determination of energy losses generated in a vibrating belt of CVT transmission

Waldemar ŁATAS[1]* **and Adam KOT**[2]

[1] Department of Applied Mechanics and Biomechanics, Faculty of Mechanical Engineering, Cracow University of Technology, Poland
[2] Department of Automotive Vehicles, Faculty of Mechanical Engineering, Cracow University of Technology, Poland

Abstract. The paper presents a proposition of the theoretical-experimental method of determination of power losses in the transversely vibrating rubber V-belt of continuously variable transmission. The article comprises the results of experimental tests conducted on a special test stand with a complete scooter drivetrain powered by a small two-stroke internal combustion engine. Such a configuration allows ensuring real CVT working conditions. A high-speed camera was used for the contactless measurement of belt vibrations and time-lapse image analysis was performed in dedicated software. An axially moving Euler–Bernoulli beam was assumed as the mathematical model. Longitudinal vibrations and nonlinear effects were omitted. Additionally, it was assumed that the belt material behaves according to the Kelvin–Voigt rheological model. Analysis of the damped free vibrations of the cantilever beam, made of the belt segment, allowed to determine the equivalent bending damping coefficient. The CVT power losses, due to bending in the rubber transmission belt, were obtained for the fixed working conditions after numerical calculations. The proposed methodology is a new approach in this research area, which allows to obtain results impossible to achieve with other measurement methods.

Key words: continuously variable transmission; moving beam vibrations; high-speed camera; power losses.

1. INTRODUCTION

Nowadays, high-speed cameras are more and more frequently used for fast-changing processes registration. The capabilities of cameras often distinctly exceed those of traditional measurement methods, and, consequently, they are applied in various research areas, such as crash tests and ballistic tests. The present paper focuses on the use of a high-speed camera to study vibration phenomena.

Paper [1] presents the method of using the Phantom V210 camera (2000 fps) and the TEMA Motion software to record the vibrations of a specialized robot gripper. The methodology proposed by the authors made it possible to confirm the occurrence of vibrations in the structure and to determine the relationships between the parameters of the robot's motion (velocity and acceleration) and the magnitude of vibrations. At the same time, attention was paid to the influence of image resolution on measurement accuracy. The tests used a point marker identified by means of image analysis software. Such a marker can also be created in the form of a grid, which allows recording the behavior of the deformable surface. This solution was presented in work [2], where the cooperation of the rubber block and the glass cylinder was analyzed in terms of vibrations generated in the friction pair as a result of the stick-slip phenomenon. The Photron FASTCAM Mini AX 100 camera, recording the image with a frequency of 6400 fps, was used. The results obtained allowed to develop a physical model of rubber surface vibrations. The tests were carried out on a specially prepared sample of a small size, which allowed to achieve the desired measurement accuracy with the available image resolution. The methodology of non-contact vibration recording using a high-speed camera is also presented in [3]. A method of image processing that allows to increase the accuracy of measurement was also proposed. The results of the tests performed with the FLARE 12M180MCX camera at the recording frequency of 200 fps were compared with the results recorded with an accelerometer (sampling frequency of 2000 Hz), manifesting very high compatibility (correlation above 99%). Also, it was noted that the accuracy of measurement depends to a much greater extent on the set size of the aperture than on the focal length. In addition, it was found that when registering low-frequency phenomena (below 15 Hz), a high-speed camera can be replaced with a much cheaper SLR camera.

Contemporary vehicles are often equipped with stepless gearboxes, known as continuously variable transmissions (CVTs). These mechanisms enable obtaining any gear ratio within a specified range, unlike traditional transmissions. As a result, much better utilization of the internal combustion engine power characteristics is possible because of engine operating in the optimal range of rotational speeds. This is beneficial for fuel consumption and car dynamics [4–6]. In modern vehicles, the push belt (steel or hybrid) CVTs have found their most

*e-mail: waldemar.latas@pk.edu.pl

Manuscript submitted 2022-12-06, revised 2023-04-26, initially accepted for publication 2023-05-30, published in October 2023.

common use; however small two-wheeled vehicles are generally equipped with rubber V-belts. This type of powertrain is significantly more reliable, simpler and cheaper than push belt solutions where an advanced ratio control system and friction pair lubrication are both needed. However, the lack of cooling in the contact area between the belt and pulley limits the torque capacity of rubber V-belt CVT and therefore this solution is dedicated only to small vehicles like scooters. It should be strongly emphasized that the main problem of rubber belt transmissions results from high power losses. The efficiency is in the range from only 50% to 80% [7], which constitutes a very low value, especially in reference to the classic toothed gears where power losses are less than 5%. Powertrain efficiency determines fuel consumption and furthermore the emission of pollutants from exhaust gases. Scooters are commonly used around the world but especially in south-east Asia. For example, they constitute 80% of the market for on-road vehicles in India [8]. Taking into account that this vehicle segment is very popular, the issue raised seems to be very important in a global sense.

Generally, the improvement of rubber V-belt CVT efficiency may be effected by the application of an advanced ratio control method or a change of belt properties, implying a change of its behavior. The second solution refers to both the contact area with the pulley (deformation and slip) and the free part of the belt (vibrations). The complexity of this problem is caused by, among others, the belt transverse and longitudinal flexibility, material hysteresis (rubber), V-shape cross-section of the belt and the variability of forces in the belt [9–13].

Issues related to modeling and testing of belt transmissions (including CVT transmissions) are up-to-date and are of interest to many researchers. In article [14], a comprehensive review of works devoted to the belt drive was made, paying particular attention to the issues of contact mechanics between the belt and pulley, fatigue life estimation and belt vibrations. Paper [15] presents a proposal for a coupled temperature-displacement analysis showing the relationship between belt slippage and its temperature. A complex numerical analysis which, however, does not make any reference to the experimental research, is presented.

The issue of vibration phenomena in belt transmission has been considered by many authors over the last several decades [16–24], but usually they did not go beyond the area of the theoretical analyses. Two main approaches to belt dynamics description are presented in the literature. If flexural rigidity can be omitted, the string model of the axially moving system is used (this approach is usually correct for long and narrow belts) [25–27]. On the other hand, one of the beam models is applied (Euler–Bernoulli, Timoshenko or Rayleigh) [28–30]. A wide overview of mathematical descriptions with both linear and nonlinear models is comprised in works [31, 32]. The presented approaches use partial differential equations (PDE) and integro-partial differential equations (IPDE).

In the present paper, the authors focus solely on the CVT power losses due to the energy dissipation in a transversely vibrating transmission rubber belt (free part). It is worth noting that the issue of the impact of belt vibrations on transmission efficiency is not explored in either theoretical or experimental terms. Transmission belt vibrations have not been considered even in extensive works dealing with CVT power losses [33, 34].

The proposed method of using a high-speed camera for the registration of vibrations in a CVT drive belt in a complete drive system of a city scooter seems to offer vast opportunities. This approach is devoid of the disadvantages of rangefinder sensors and, additionally, it allows recording the belt section (the measurement does not concern only selected points).

The real working conditions of the belt transmission were ensured by using a real drive source (not an electric motor, as usually). This is especially important from the point of view of the analysis of vibrational phenomena because the engine is a wide-band excitation source.

The use of a high-speed camera for the determination of power losses in a transversely vibrating belt is a new method in this research area. However, the application of a high-speed camera in the analysis of belt movement was proposed in work [35].

The present paper shows the complete methodology and contains the experimental research and theoretical approach. The power loss determination on the basis of the obtained experimental data is also explained. An axially moving Euler–Bernoulli beam was used as the mathematical model, made of a material behaving according to the Kelvin–Voigt rheological model. Moreover, the method of determining the coefficient describing the damping properties of the belt is also discussed.

Based on the measurement results obtained on the test stand built, exemplary results of calculations of the dissipated power, for various rotational speeds, in the DAYCO 17.5 × 765 transmission belt performing transverse vibrations are presented.

2. PHYSICAL STRUCTURE OF TRANSMISSION BELT

Due to the non-homogeneity of a given cross-section (Fig. 1) and the variability of the cross-sectional area along the belt length, theoretical determination of values of the physical parameters describing the behavior of the moving vibrating transmission belt would be very complex. Numerical calculations of these values, for example with the use of FEM, would also be time-consuming. Both methods would require knowledge of the material constants of each of the belt components, i.e. nylon cord, rubber core and fiber layer.

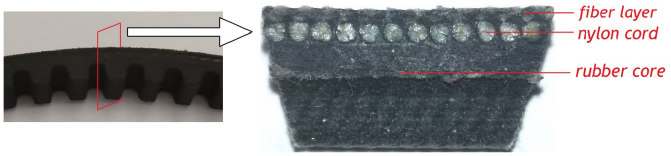

Fig. 1. Cross-section of a CVT rubber V-belt [DAYCO 17.5 × 765]

Additionally, it would be necessary to know the way these elements interact with each other, which would require knowledge of the production process technology.

The observations showed that despite the heterogeneous structure small vibrations of the cantilever beam, made of the

transmission belt section, disappear with a very good approximation in accordance with the damping described by the linear Kelvin–Voigt rheological model. Despite various energy dissipation phenomena occurring in the axially moving and vibrating transmission belt, their quantitative description using the one equivalent factor is therefore fully justified.

3. MATHEMATICAL MODEL OF TRANSMISSION BELT VIBRATIONS

The Kelvin–Voigt and SLS (standard linear solid) models were used traditionally to describe the material damping of the beam. Employing the K–V constitutive relation, two different approaches were used: the viscoelastic model with neglected steady dissipation term due to the axial motion of the beam [29], and the model with the steady dissipation included [36]. In the first model the constitution relation is given by: $\sigma = E\varepsilon + \alpha\varepsilon_t$, whereas the second model assumes the steady dissipation term resulting from the material time derivative.

The paper utilizes the second model, the justification for which is given later in Section 5, where the formula for the power dissipated in the beam due to bending is provided.

The constitutive stress-strain relation is given by:

$$\sigma = E\varepsilon + \alpha\left(\varepsilon_t + V\varepsilon_x\right), \tag{1}$$

where E and α are Young's modulus and the viscous damping coefficient, and V is the transport velocity of the axially moving belt.

Because the belt is non-homogeneous, the equivalent coefficients (averaged along the belt length) are introduced: $\overline{\rho A}$, $\overline{EI}$, $\overline{\alpha I}$, where ρ represents density while A and I are cross-section area and area moment of inertia, respectively.

The mathematical model applied is an axially moving Euler–Bernoulli beam with time dependent velocity, and the nonlinear effects and longitudinal vibrations are ignored.

A formula for the bending moment M can be obtained from (1):

$$M = \overline{EI}w_{xx} + \overline{\alpha I}\left(w_{xxt} + Vw_{xxx}\right), \tag{2}$$

where expressions in (1) and (2) resulted from the material time derivative applied.

For the abovementioned assumptions, the equation of the transverse motion of the moving belt is given by:

$$\overline{\rho A}\left(w_{tt} + \dot{V}w_x + 2Vw_{xt} + V^2w_{xx}\right) - T_0w_{xx} + \overline{EI}w_{xxxx} + \overline{\alpha I}\left(w_{xxxt} + Vw_{xxxxx}\right) = 0, \tag{3}$$

where $w(x,t)$ denotes transverse displacement, x and t are axial and time coordinates, and T_0 is static tension, assumed to be constant along the belt.

The belt vibration equation (3) is a homogeneous equation. The direct cause of vibrations is parametric excitation resulting from the fact that axial velocity of the belt V is not constant over time. This velocity depends on instantaneous angular velocity and the drive pulley radius, and it is a periodic function with a period equal to the time of one rotation of the pulley related to the value of nominal rotational speed.

Taking into account the difference in the terms of (3): $\left(\overline{\rho A}V^2 - T_0\right)w_{xx}$, it can be seen that the expression $\overline{\rho A}V^2$ can be treated as a periodic disturbance of constant tension force T_0, which is the cause of parametric excitation of vibrations.

4. DETERMINATION OF DAMPING COEFFICIENT OF TRANSMISSION BELT

In (3), there are several parameters affecting the vibrations of the moving belt. Experimental tests were carried out on a new DAYCO 17.5×765 transmission belt. The equivalent longitudinal inertia coefficient: $\overline{\rho A} = 0.13$ kg/m is the average linear density of the belt. The equivalent bending stiffness: $\overline{EI} = 8.99 \cdot 10^{-3}$ Nm^2 was determined by measuring deflection of a cantilever beam, made of the belt fragment, under the applied concentrated force. The method of determining the equivalent coefficient $\overline{\alpha I}$, on which the value of the energy dissipated due to bending depends, is briefly presented below.

The equivalent bending damping coefficient $\overline{\alpha I}$ can be determined based on the analysis of the damped free vibrations of the cantilever beam, made of the belt segment. The vibration measuring stand is presented in Fig. 2 – in order to avoid the influence of gravity on the deflection line, the vibrations of the belt occur in the horizontal plane. The measurement was conducted by two (for verification) optical distance Baumer FADK 14U4470/S14/IO sensors (measurement range: 50÷400 mm, accuracy: 0.1 mm).

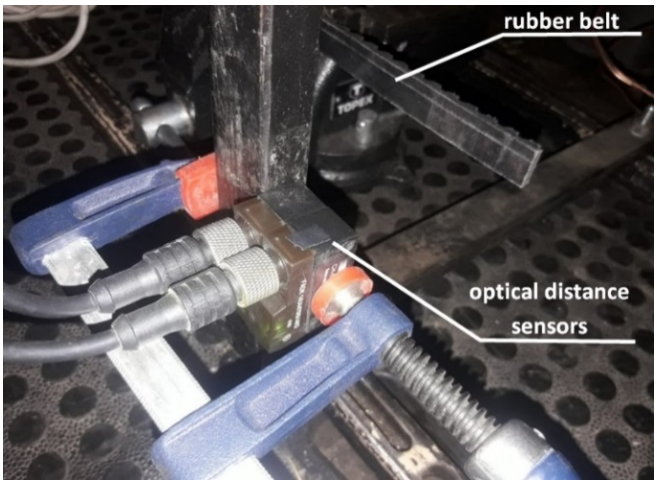

Fig. 2. Measurement stand of transmission belt segment vibrations [41] (this figure is copyrighted material and is excluded from the open access license)

Calculation of coefficient $\overline{\alpha I}$ is based on the determination of the viscous damping coefficient $2h$ of the equivalent vibrating discrete system, with one degree of freedom (Fig. 3), described by the equation of motion:

$$m\ddot{y} + 2h\dot{y} + ky = 0, \tag{4}$$

where y is the displacement of the cantilever beam end point.

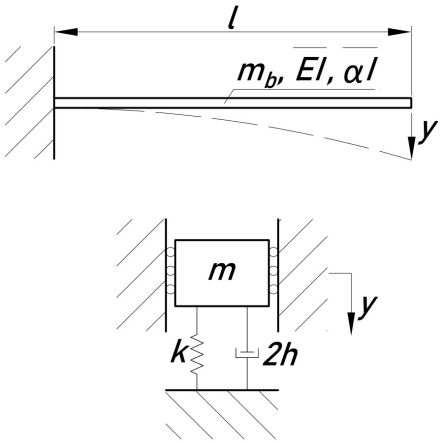

Fig. 3. Cantilever beam and equivalent 1.d.o.f. system

The first mode of beam vibrations was assumed as the line of static deflection of the cantilever beam under concentrated force applied at its end. Comparison of the kinetic energies of the beam and the equivalent 1.d.o.f. system gives the following:

$$m = \frac{33}{140} m_b \,, \tag{5}$$

where m_b is the mass of the vibrating section of the belt with a length of $l = 0.150$ m, equal to: $m_b = 0.020$ kg.

The plots in Fig. 4 show examples of displacement waveforms of the cantilever beam end point.

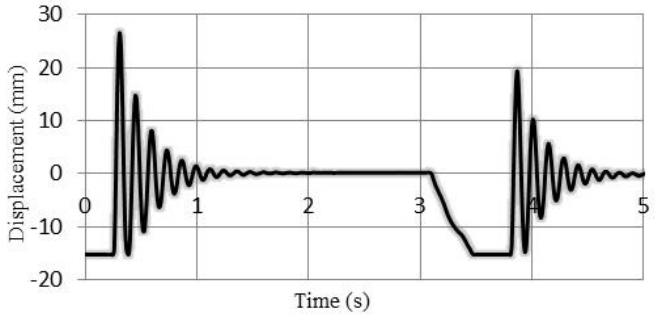

Fig. 4. Transverse displacement waveforms measured at end point of cantilever beam

On the basis of these waveforms, the logarithmic decrement of damping was determined. After simple calculations, the following value of coefficient h ((4)) was obtained:

$$h = 0.022 \ \frac{\text{kg}}{\text{s}} \,. \tag{6}$$

Comparing the energy dissipated in the cantilever beam of length l with the energy dissipated in the damper of the 1.d.o.f equivalent system (during one vibration period T):

$$\overline{\alpha I} \int_0^l \int_0^T (w_{xxt})^2 \, \mathrm{d}x \mathrm{d}t = 2h \int_0^T \dot{y}^2 \, \mathrm{d}t, \tag{7}$$

the following formula was obtained:

$$\overline{\alpha I} = \left(\frac{35}{214} \right) l^3 h = 1.214 \cdot 10^{-5} \ \frac{\text{kg m}^3}{\text{s}} \,. \tag{8}$$

5. POWER DISSIPATED IN MOVING BELT DUE TO VIBRATIONS

Only transverse vibrations were considered in the work, whereas the influence of longitudinal belt vibrations on energy dissipation was omitted. Taking into account only the energy dissipated during belt bending is justified by its composite structure. The nylon cord (Fig. 3) is characterized by distinctly larger stiffness than the rubber core where energy dissipation takes place. The deformations in the rubber resulting from stretching or compression of the belt are negligibly small (in the tested case) in relation to the deformations resulting from bending.

The work W of internal forces resulting from bending on the $[l_1, l_2]$ belt section during the time interval $[t_1, t_2]$ is given by the formula below:

$$W = \int_{l_1}^{l_2} \int_{t_1}^{t_2} M \dot{\chi} \, \mathrm{d}x \mathrm{d}t, \tag{9}$$

where M is the bending moment given by (2) and χ is beam curvature: $\chi = w_{xx}$. Applying the material time derivative yields:

$$\dot{\chi} = w_{xxt} + V w_{xxx} \,. \tag{10}$$

The average power D of the energy dissipated due to bending in the moving transmission belt on the $[l_1, l_2]$ section in the time interval $[t_1, t_2]$ is given by the following formula:

$$D = \frac{\overline{\alpha I}}{t_2 - t_1} \int_{l_1}^{l_2} \int_{t_1}^{t_2} (w_{xxt} + V w_{xxx})^2 \, \mathrm{d}x \mathrm{d}t. \tag{11}$$

Formula (11) justifies the use of the K–V model (1) with the material derivative applied. One can imagine steady (e.g. kinematically imposed) belt movement in which w_{xxt} is always zero, but the selected belt element would be bent during this movement, causing energy dissipation (due to component $V w_{xxx}$ in (11)).

For the matrix of positions $[w_{ik}]$ obtained from the measurements, where $w_{ik} = w(x_i, t_k)$ denotes the positions of the point with coordinate x_i at the time t_k, interpolation of the w_{xxt} and w_{xxx} derivatives is performed, allowing the dissipated power to be calculated according to (11).

In the numerical calculations, both for the interpolation and the calculation of the double integral, the numerical procedures of the IMSL® C package are utilized [37].

6. METHODS OF MEASUREMENTS OF MOVING BELT VIBRATIONS

Measurement of vibrations under real working conditions is crucial from the point of view of assessing their causes and factors influencing their magnitude. The method of registering belt

vibrations should not affect its behavior. Therefore, only non-contact methods, such as image registration or optical proximity sensors, can be used here. The use of optical rangefinders is a relatively less complicated and cheaper approach, but it does not provide full information about the behavior of the tested object when only a single sensor is used. In the literature, there are mentions of some attempts to locally record belt vibrations using laser sensors [38–40] and electrostatic sensors [38]. The research presented in the abovementioned works was carried out on model objects, and was thus devoid of all the inconveniences associated with the real drive system, such as lack of assembly space.

CVT rubber drive belts for small two-wheelers are not high-accuracy components. The incompletely vulcanized top layer of the fabric causes the surface of the back of the belt to be neither smooth nor monochromatic. The resulting measurement difficulties are visible already at the stage of static calibration of the sensor. In addition, in the case of sensors of this type, it is problematic to constantly change the angular orientation of the reflecting surface, which is a natural consequence of the undulation of the belt. As a result, this can contribute to a significant reduction in measurement accuracy. A certain danger resulting from the use of a single sensor (local measurement) is the possibility of placing it near a vibration node.

In view of the above, the analysis of belt vibrations based on the measurement with the optical sensor in question may be subject to a relatively large error. It is therefore fully justified to use more advanced tools, such as high-speed cameras. Work [39] presents the behavior of a poly V-belt recorded with a high-speed camera, which, however, was not the basis for a deeper analysis.

The main advantage of vibration measurements using a high-speed camera is the ability to determine the positions of many points along the belt at the same moment of time, which is not possible using a single optical sensor. This allows to achieve a convenient approximation or interpolation of displacement functions and their spatial derivatives.

The applied method of registering drive belt vibrations is not without its limitations. The use of a high-speed camera is possible only in bench tests, which is a significant difficulty in testing vehicle drive systems, because it necessitates the preparation of an object that accurately reflects real operating conditions. Drive belts in vehicles usually operate in closed housings, so it is necessary to prepare observation windows or dismantle the covers. Proper positioning of the camera (distance and angular orientation relative to the object) requires a specific working space, which excludes recording in the absence of free access to the belt. The high recording frequency, which is key for the considered angular velocities of the drive motor, increases the accuracy of the measurement but at the same time it implies serious difficulties related to the collection of extensive footage. For example, a 2-minute HD-SDI recording requires 200 GB of disk space. A frame-by-frame analysis of the collected data is a time-consuming process as with the current level of dedicated software it is not possible to automatically track a moving object with variable geometry, such as an undulating belt. The available tools, on the other hand, allow, for example, for automatic analysis of angular vibrations of the pulley.

The accuracy of measurement depends on the resolution of the recording and the dimensions of the object (or its fragment) in the frame. In the case of the analyzed belt transmission of a city scooter and the recording devices used, a measurement resolution of about 0.20 mm was obtained, which is a satisfactory value from the point of view of the observed phenomenon (the exact scale factor resulting from the image resolution and the actual size was 0.186 mm/pix). Although the theoretical measurement resolution of the optical sensors is lower (0.10 mm for Baumer FADK sensors), their high sensitivity to color and structural heterogeneity of the belt introduces a significant measurement error estimated at ± 1 mm (according to own research).

Regardless of the measurement method, the short-term torsional vibrations of the belt pose a problem, which may result in an incorrect assessment of the actual displacement of the belt. Comparing the cost of the equipment used in the implementation of research tests with non-contact methods, it should be noted that it is many times higher in the case of a high-speed camera, even assuming the use of a dozen optical sensors. On the other hand, a high-speed camera provides incomparably more extensive research material, and the cost of research can be significantly reduced by using the offers of specialized companies providing services in this area.

7. TEST STAND FOR MEASUREMENTS OF TRANSMISSION BELT VIBRATIONS

The experimental research was conducted on a test stand equipped with a complete drive system of the TGB 101S scooter powered by a two-stroke internal combustion engine (3.5 kW) with a swept volume of 49 cm^3. The scheme of the test stand is shown in Fig. 1 and the method of conducting the experiment with the use of a high-speed camera is shown in Fig. 5.

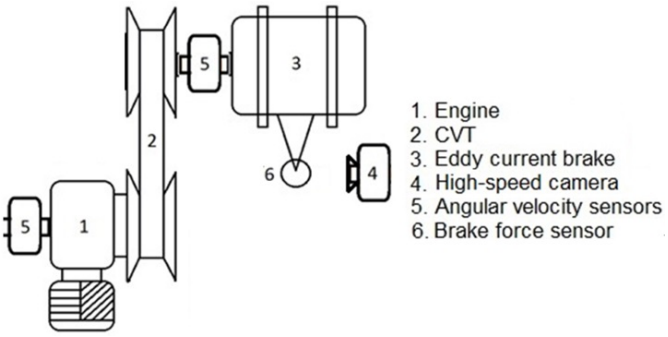

Fig. 5. Test stand scheme [41] (this figure is copyrighted material and is excluded from the open access license)

The professional Phantom VEO 710S high-speed camera, shown in Fig. 6, was used during the experiment. The image was recorded in HD-SDI quality at the resolution of 1280×720. The registration frequency was 8300 fps, so at the maximum considered engine speed of 6000 rev/min, it made it possible to

record an image every 4.3° of a rotation angle of the crankshaft. The camera's lens has to be situated orthogonally to the plane of the belt movement so it is impossible to capture the entire transmission because of the location of the eddy current brake. Before starting the recording of the footage, the tested object was properly prepared. In order to obtain the best background contrast for the moving belt, the body of the gear was given a white color (Fig. 7), which is of particular importance when the high-speed camera used records the image in shades of grey.

Figures 8a–8d show the behavior of the belt during a rotation of the crankshaft at rotational speed of 4560 rev/min (i.e. nominal average speed).

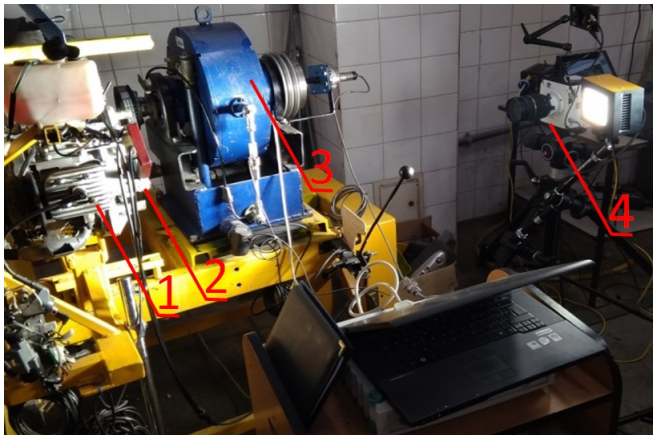

Fig. 6. View of test stand with Phantom VEO 710S high-speed camera (1 – engine, 2 – CVT, 3 – eddy current brake, 4 – camera) [41] (this figure is copyrighted material and is excluded from the open access license)

Fig. 7. Body of CVT gear prepared for recording footage

a)

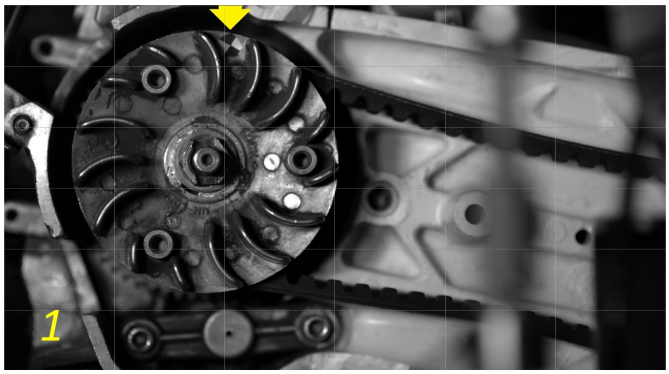

b)

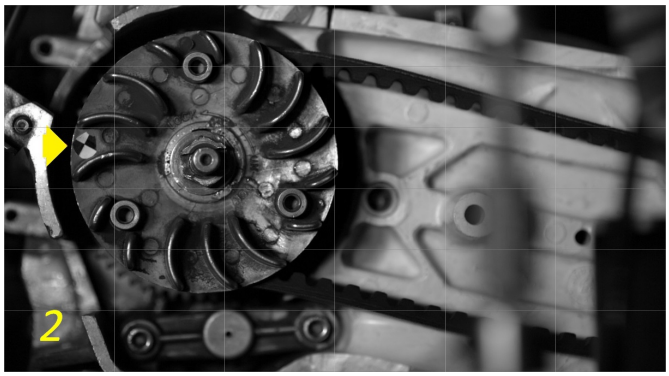

c)

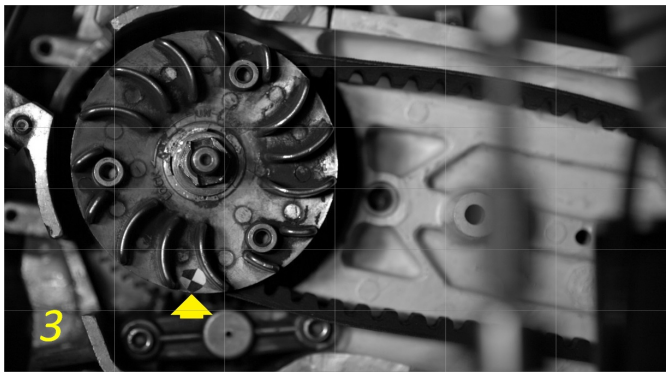

d)

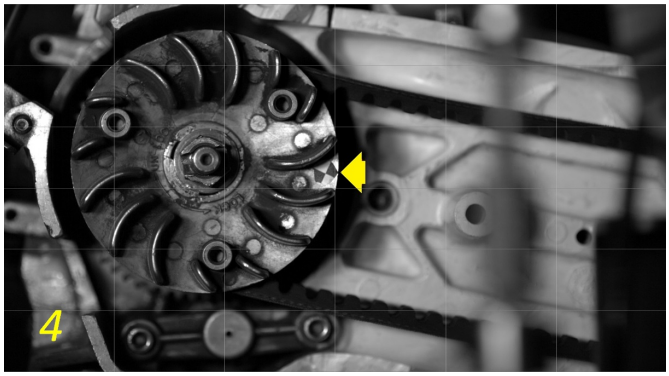

Fig. 8. Belt vibration during single drive pulley revolution; rotational speed of 4560 rev/min

8. DETERMINATION OF POWER DISSIPATED DURING TRANSMISSION OPERATION

The TEMA Motion 4.2 software was used for time-lapse image analysis. The professional environment used for image analysis in 2D mode provides the ability to track and save the coordinates of a distinguished small element of the frame, which allows for far-reaching automation of the image analysis process. However, the studied problem of drive belt vibrations required capturing a larger element with variable geometry, where software tracking of selected points turned out to be impossible. Thus, there was a need for manual, frame-by-frame analysis of the recorded image. The program allows saving the coordinates of the selected points in a predefined coordinate system. The coordinate system has been linked to the axis of the drive wheel visible in the frame. The belt tracks, for both tight and slack sides, were registered by selecting the points constituting the outside edge of the belt (on the cord side) and equally spaced from each other (14 points on each belt side – Fig. 9).

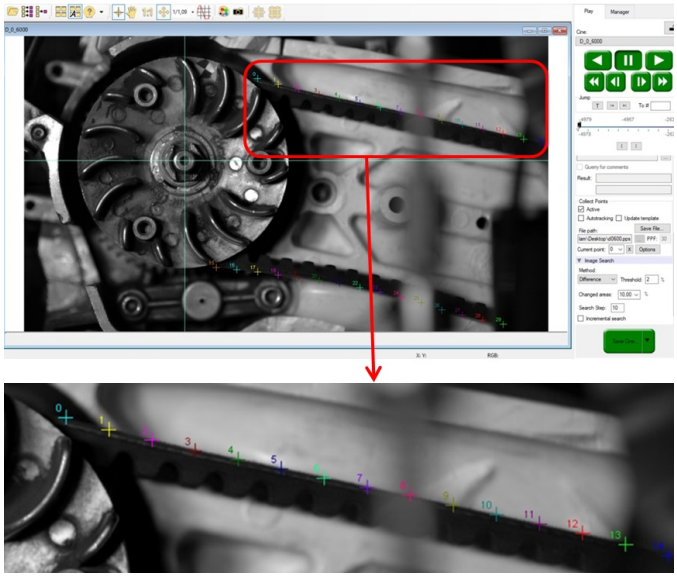

Fig. 9. Belt vibrations – measurement points. View in TEMA Motion 4.2 software

As a result, the position of the belt in the transverse direction was presented in the form of tabulated functions of two variables (individual for tight and slack belt side), i.e. time and longitudinal coordinate. The tests were performed under fixed working conditions defined by the transmission ratio (0.9), throttle position (100%) and engine rotational speed (3 values being considered: 3150, 4560 and 6000 rev/min).

The time-lapse analyses were conducted for ten subsequent crankshaft revolutions, and constitute an extension of the results presented in paper [41].

Taking into account the considered relatively long recording time (10 revolutions of the crankshaft) and the high recording frequency of the high-speed camera (8300 fps), it was decided that every 10th frame should undergo analysis due to the need for manual time-lapse processing of the recording. It should be noted, however, that this has no adverse effect on the accuracy of mapping the transverse movement of the belt, even at high engine speed, as the step obtained for the time variable was 1.2 ms.

Figure 9 shows the shape of the belt during the transmission operation at a given moment of time, with marked points, the positions of which (i.e. distances from the horizontal axis) are determined with the use of the high-speed camera. The distances between the projections of these points on the horizontal axis are equal to 9.32 mm. It should be emphasized that in the following moments of time, as a result of axial movement, these points indicate physically different places of the belt.

Based on the measurements, the matrix of positions $[\tilde{w}_{ik}]$ is determined, where $\tilde{w}_{ik} = \tilde{w}(\tilde{x}_i, t_k)$ denotes the position of the point with the coordinate $\tilde{x}_i$ at the time t_k. The positions $\tilde{w}_{ik}$ and the $\tilde{x}_i$ coordinates are transformed (by rotation) into the system whose abscissa axis is parallel to the tangent to the transmission pulleys (i.e. into w_{ik} and x_i). This allows determining the power dissipated in a moving transmission belt according to the method described in Section 4.

Although the equivalent damping coefficient for bending has been determined on the basis of tests at room temperature (Section 4), it can be used in the calculation of the dissipated power (11) as the measurements made with a pyrometer have shown that the temperature of the belt increases only by a few degrees Celsius. Such an increase in temperature certainly does not cause any considerable changes in the physical properties of the belt material.

Table 1 presents the average values (with standard deviation) of power dissipated in the transmission belt for rotational speed (i.e. nominal average speed) of the drive pulley equal to: 3150, 4560 and 6000 rev/min, both for the tight side and the slack side. For the listed rotational speed values, the average axial velocity values are equal to: 13.85, 20.05 and 26.38 m/s, respectively.

Table 1

Average power in Watts (with standard deviation) dissipated in transmission belt for various rotational speeds

	$n = 3150$ rev/min	$n = 4560$ rev/min	$n = 6000$ rev/min
Tight belt side (upper fragment)	4.66 (0.62)	38.17 (2.83)	12.14 (2.63)
Slack belt side (lower fragment)	50.21 (1.57)	24.35 (2.56)	151.88 (8.26)
Sum	**54.87**	**62.52**	**164.02**

During the numerical calculations, it was assumed that the location of each belt point may take any value in the range of $(\tilde{w}_{ik} - 0.1$ mm, $\tilde{w}_{ik} + 0.1$ mm) with the same probability. Therefore, Table 1 presents the expected values of dissipated power (together with standard deviations). The accuracy of numerical calculations was tested on an example sinusoidal function for which the results of approximate numerical integration could be compared with the exact results of analytical calculations.

In all cases, the calculations were made for the same lengths of the belt segments (the tight side and the slack side) equal to approximately $\Delta l = 0.121$ m. The dimensions of matrix $[w_{ik}]$ are 14×163.

9. ADDITIONAL RESULTS AND REMARKS REGARDING VIBRATIONS IN MOVING TRANSMISSION BELT

Table 2 shows the first three approximate natural frequencies of the moving belt for three tested values of the nominal rotational speed. The constant tensile force values were obtained on the basis of forces in the tight and slack sides, resulting from the drive torque measured on the output pulley.

Table 2
Approximate natural frequencies of moving belt

	$n = 3150$ rev/min $f_0 = 52.5$ Hz	$n = 4560$ rev/min $f_0 = 76.0$ Hz	$n = 6000$ rev/min $f_0 = 100.0$ Hz
Tight belt side (upper fragment)	$T_0 = 98$ N $f_1 = 41.1$ Hz $f_2 = 88.1$ Hz $f_3 = 146.6$ Hz	$T_0 = 121$ N $f_1 = 35.2$ Hz $f_2 = 77.9$ Hz $f_3 = 135.8$ Hz	$T_0 = 130$ N $f_1 = 20.5$ Hz $f_2 = 52.1$ Hz $f_3 = 105.1$ Hz

The frequencies were determined on the basis of the approximate formula derived in paper [42]; details of the calculations for the discussed case are included in paper [35]. The basic assumptions were low (and constant) axial velocity, small bending stiffness, neglecting the damping and the free support boundary conditions. The following additional values of parameters were used in the calculations: length of free part of the belt – 0.255 m; radius of the drive pulley – 0.042 m.

Figure 10 shows, for the rotational speed equal to 4560 rpm, the velocity frequency spectrum of the belt point located at the distance of 70 mm from the left belt-pulley contact point at the tight part of the belt. The two main extremes on the graph are related to the fact that the conditions for parametric resonance are met with adequate approximation, i.e.: $f_0 = 76.0$ Hz ≈ 77.9 Hz $= f_2$; $2f_0 = 152.0$ Hz ≈ 154.8 Hz $= 2f_2$.

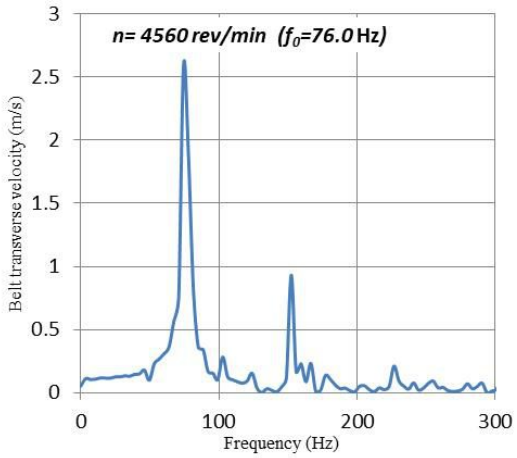

Fig. 10. Transverse velocity spectrum for rotational speed of 4560 rpm, velocity measured at 70 mm from left belt-pulley contract point at tight (upper) part of belt

Despite the potential adverse effect on the operation of the transmission, resonance does not necessarily mean large values of dissipated energy resulting from transverse vibrations of the belt. Dissipated power does not depend on the displacement values, but on their spatial and time derivatives (11).

A more accurate analysis of the vibrations of the moving belt must take into account the fact that with large amplitudes of motion, a part of the belt may wind up on the drive pulley. As a result, at a fixed moment, transverse vibrations are performed only by the part of the belt (which can change its length) between both pulleys of the transmission. Such an analysis would require other than free support of the boundary conditions.

10. DISCUSSION

The presented values of power losses concern only the part of the belt captured by the high-speed camera. Taking into account the ratio of the belt visible part length to the fragments covered up by pulleys and eddy current brake, the total power losses resulting from belt vibrations are, according to the authors' estimates, about 30% higher. However, it should be noted that the received values correspond with efficiency of the identical CVT, where overall power loss (considering belt slip, hysteresis, etc.) under similar working conditions is in the range of 500–1000 W [7]. Thus, approximately 10–15% of the power loss is due to dissipation in the transversely vibrating belt.

In general, the slack belt side is responsible for greater power loss. The greater value of the power dissipated on the tight side for $n = 4560$ rev/min is related most probably to the possible parametric resonance phenomenon.

The dissipation of energy in the moving belt is associated with the release of heat that must be transferred to the surroundings. Assuming forced convection and taking into account the estimated value of the heat transfer coefficient between rubber and air, and also considering the belt surface area, it was determined that the temperature increase of the belt above ambient temperature is over a dozen degrees. This estimate is sufficient to conclude that the heat generated during the vibration will not cause the belt temperature to rise excessively. Accurate simulation of thermodynamic phenomena, which is not the purpose of this paper, would be complex and time-consuming.

11. CONCLUSIONS

The power losses of the rubber belt CVT are generally categorized into the following main terms: sliding losses between belt and pulleys; hysteresis of the belt material in both the longitudinal and transverse directions; work required to engage and disengage the belt in and from the pulley [33]. In the literature, vibration phenomena are not identified as a factor significantly affecting efficiency of the rubber V-belt CVT.

The presented test results do not contradict this approach to the causes of power losses. On the other hand, the obtained values of power dissipated in the belt are not marginal and constitute a space for improving the efficiency of this type of trans-

mission. On a global scale, even several percent of improvement in CVT efficiency has a measurable influence in the context of fuel consumption and further in the context of pollutant emission from exhaust gases [43].

Despite the already discussed difficulties in accurately determining the power losses arising in the transversely vibrating transmission belt, it should be noted that no results were obtained that would exclude the correctness of the method used. Moreover, the received values of the power lost in the vibrating belt correspond to the total power loss. From the quantitative point of view, the results obtained so far should be treated as estimates which are reasonable from the point of view of engineering practice. Further work should be aimed at validating the proposed methodology, which is extremely difficult due to the complexity of the subject matter. It is worth noting that the presented methodology may find broader technical application, and therefore, according to the authors, the development of the selected research problem is fully justified.

The approach presented in the paper to the determination of losses in CVTs resulting from vibrations of the transmission belt on the basis of displacement measurements with a high-speed camera is innovative, and has not yet been used in these types of problems. The results obtained indicate that the adopted new methodology is correct and it allows for the estimation of power dissipated by the vibrating belt.

Further research in this area is expedient. It seems particularly advisable to compare the losses for different belts (different manufacturers' belts are commercially available) and for variant working conditions (transmission ratio, engine speeds). This will make it possible to distinguish the parameters particularly beneficial for the minimization of power losses caused by belt vibrations. The next stage of the research will also include theoretical analysis requiring solving the equation which describes the transverse vibrations of the moving belt.

REFERENCES

[1] W. Kaczmarek, S. Borys, J. Panasiuk, M. Siwek, and P. Prusaczyk, "Experimental study of the vibrations of a roller shutter gripper," *Appl. Sci.*, vol. 12, no. 19, p. 9996, 2022, doi: 10.3390/app12199996.

[2] F. Kuang, X. Zhou, J. Huang, H. Wang, and P. Zheng, "Machine-vision-based assessment of frictional vibration in water-lubricated rubber stern bearings," *Wear*, vol. 426–427, pp. 760-769, 2019, doi: 10.1016/j.wear.2019.01.087.

[3] C. Peng, C. Zeng, and Y. Wang, "Camera-based micro-vibration measurement for lightweight structure using an improved phase-based motion extraction," *IEEE Sens. J.*, vol. 20, no. 5, pp. 2590–2599, 2020, doi: 10.1109/JSEN.2019.2951128.

[4] B. Bonsen, M. Steinbuch, and P.A. Veenhuizen, "CVT ratio control strategy optimization," *2005 IEEE Vehicle Power and Propulsion Conference*, 2005, doi: 10.1109/VPPC.2005.1554561.

[5] R. Pfiffner, L. Guzzela, and C.H. Onder, "Fuel–optimal control of CVT powertrains," *Control Eng. Pract.*, vol. 11, no. 3, pp. 329–336, 2003, doi: 10.1016/S0967-0661(02)00219-8.

[6] W. Grzegożek, M. Szczepka, and A. Kot, "The analysis of applying CVT gear ratio rate control for scooter efficiency improvement," *Asian J. Appl. Sci. Eng.*, vol. 6, no. 2, pp. 73–80, 2017.

[7] A. Kot, W. Grzegożek, and W. Szczypiński-Sala, "The analysis of an influence of rubber V-belt physical properties on CVT efficiency," *IOP Conf. Ser.-Mat. Sci.*, vol. 421, no. 2, p. 022017, 2018, doi: 10.1088/1757-899X/421/2/022017.

[8] G. Bhowmick, T. Sahoo, A. Bhat, G. Mathur, and D. Gambhir, "Approach for CO_2 reductioning in India's automotive sector," *SAE Int.*, vol. 28, p. 2388, 2019, doi: 10.4271/2019-28-2388.

[9] T.C. Firbank, "Mechanics of the belt drive," *Int. J. Mech. Sci.*, vol. 12, no. 12, pp. 1053–1063, 1970, doi: 10.1016/0020-7403(70)90032-9.

[10] M. Cammalleri, "A new approach to the design of speed-torque-controlled rubber V-belt Variator," *Proc. Inst. Mech. Eng. Part D-J. Automob. Eng.*, vol. 219, pp. 1413–1427, 2005, doi: 10.1243/095440705X35080.

[11] G. Julió and J.-S. Plante, "An experimentally – validated model of rubber-belt CVT mechanic," *Mech. Mach. Theory*, vol. 46, no. 8, pp. 1037–1053, 2011, doi: 10.1016/j.mechmachtheory.2011.04.001.

[12] G.B. Gerbert, "Belt slip – a unified approach," *J. Mech. Design,* vol. 118, no. 3, pp. 432–438, 1996, doi: 10.1115/1.2826904.

[13] K. Kubas, "A two-dimensional discrete model for dynamic analysis of belt transmission with dry friction," *Arch. Mech. Eng.*, vol. 61, no. 4, pp. 571–593, 2014, doi: 10.2478/meceng-2014-0033.

[14] H. Zhu, W. Zhu, and W. Fan, "Dynamic modeling, simulation and experiment of power transmission belt drives: A systematic review," *J. Sound Vib.*, vol. 491, no. 1, pp. 1–40, 2021, doi: 10.1016/j.jsv.2020.115759.

[15] Z. Yu, Y. Cui, Q. Zhang, J. Liu, and Y. Qin, "Thermo-mechanical coupled analysis of V-belt drive system via absolute nodal coordinate formulation," *Mech. Mach. Theory*, vol. 174, no. 1, p. 104906, 2022, doi: 10.1016/j.mechmachtheory.2022.104906.

[16] I.V. Andrianov and W.T. Horrsen, "On the transversal vibrations of a conveyor belt: Applicability of simplified models," *J. Sound Vib.*, vol. 313, no. 3, pp. 822–829, 2008, doi: 10.1016/j.jsv.2007.11.053.

[17] J. Ding and Q. Hu, "Equilibria and free vibration of a two-pulley belt-driven system with belt bending stiffness," *Math. Probl. Eng.*, p. 907627, 2014, doi: 10.1155/2014/907627.

[18] E.-W. Chen, H. Lin, and N. Ferguson, "Experimental investigation of the transverse nonlinear vibration of an axially travelling belt," *J. Vibroeng.*, vol. 18, no. 8, pp. 4885–4900, 2016, doi: 10.21595/jve.2016.17341.

[19] V. Ravindra, C. Padmanabhan, and C. Sujatha, "Static and free vibration studies on a pulley belt system with ground stiffness," *J. Braz. Soc. Mech. Sci.*, vol. 32, no. 1, pp. 61–70, 2010, doi: 10.1590/S1678-58782010000100009.

[20] R. Zhang, X. Si, W. Yang, and N. Wang, "Analysis of resonance reliability for synchronous belt transmission with transverse vibration," *J. Vibroeng.*, vol. 16, no. 2, pp. 891–900, 2014.

[21] L. Kong and R.G. Parker, "Steady mechanics of belt-pulley systems," *J. Appl. Mech.*, vol. 72, no. 1, pp. 25–34, 2005, doi: 10.1115/1.1827251.

[22] H. Ding, C.W. Lim, and L.-Q. Chen, "Nonlinear vibration of a traveling belt with non-homogeneous boundaries," *J. Sound Vib.*, vol. 424, pp. 78–93, 2018, doi: 10.1016/j.jsv.2018.03.010.

[23] M. Kim and J. Chung, "Dynamic analysis of a pulley-belt system with different pulley radii and support stiffness," *J. Mech. Sci. Technol.*, vol. 32, no. 12, pp. 5597–5613, 2018, doi: 10.1007/s12206-018-1106-8.

[24] D. Schnürer and H.J. Holl, "Transversal vibrations of a toothed belt in linear drives during operation," *Proc. Appl. Math. Mech.*, vol. 20, no. 1, p. e202000026, 2021, doi: 10.1002/pamm.202000026.

[25] J. Moon and J.A. Wickert, "Non-linear vibration of power transmission belts," *J. Sound Vib.*, vol. 200, no. 4, pp. 419–431, 1997, doi: 10.1006/jsvi.1996.0709.

[26] W. Łatas, "Active vibration suppression of axially moving string via distributed force," *Vib. Phys. Syst.*, vol. 3, no. 2, pp. 2020215-1–2020215-8, 2020, doi: 10.21008/j.0860-6897.2020.2.15.

[27] P. Lad and V. Kartik, "Stability transitions of an axially moving string subjected to a distributed follower force," *Proc. R. Soc. A.*, vol. 474, no. 2213, p. 20170779, 2018, doi: 10.1098/rspa.2017.0779.

[28] F. Pellicano and F. Vestroni, "Nonlinear dynamics and bifurcations of an axially moving beam," *J. Vib. Acoust.*, vol. 122, pp. 21–30, 2000, doi: 10.1115/1.568433.

[29] L.Q. Chen and X.D. Yang, "Stability in parametric resonance of axially moving viscoelastic beams with time-dependent speed," *J. Sound Vib.*, vol. 284, no. 3, pp. 879–891, 2005, doi: 10.1016/j.jsv.2004.07.024.

[30] D. Karlicic, M. Cajic, S. Paunović, and S. Adhikari, "Periodic response of a nonlinear axially moving beam with a nonlinear energy sink and piezoelectric attachment," *Int. J. Mech. Sci.*, vol. 195, 2021, doi: 10.1016/j.ijmecsci.2020.106230.

[31] P.T. Pham and K.S. Hong, "Dynamic models of axially moving systems: A review," *Nonlinear Dyn.*, vol. 100, pp. 315–349, 2020, doi: 10.1007/s11071-020-05491-z.

[32] H. Zhu, W.D. Zhu, and W. Fan, "Dynamic modeling, simulation and experiment of power transmission belt drives: A systematic review," *J. Sound Vib.*, vol. 491, 2021, doi: 10.1016/j.jsv.2020.115759.

[33] L. Bertini, L. Carmignani, and F. Frendo, "Analytical model for the power losses in rubber V-belt continuously variable transmission (CVT)," *Mech. Mach. Theory*, vol. 78, pp. 289–306, 2014, doi: 10.1016/j.mechmachtheory.2014.03.016.

[34] T.F. Chen and C.K. Sung, "Design considerations for improving transmission efficiency of rubber V-belt CVT," *Int. J. Vehicle Des.*, vol. 24, no. 4, pp. 320–333, 2000, doi: 10.1504/IJVD.2000.005195.

[35] A. Kot and W. Łatas, "Experimental and theoretical investigation of CVT rubber belt vibrations," *Open Eng.*, vol. 11, pp. 1196–1206, 2021, doi: 10.1515/eng-2021-0121.

[36] E.M. Mockensturm and J.P. Guo, "Nonlinear vibration of parametrically excited, viscoelastic, axially moving strings," *J. Appl. Mech.*, vol. 72, no. 3, pp. 374–380, 2005, doi: 10.1115/1.1827248.

[37] *IMSL® C Numerical Libraries*, Visual Numerics, Inc.

[38] Y. Hu, Y. Yan, L. Wang, and X. Qian, "Non-contact vbration monitoring of power transmission belts through electrostatic sensing," *IEEE Sens. J.*, vol. 16, no. 10, pp. 3541–3550, 2016, doi: 10.1109/JSEN.2016.2530159.

[39] L. Manin and F. Besson, G. Michon, and R. Dufour, "Experimental investigation on the dynamic characteristics and transverse vibration instabilities of transmission belts," *16ème Colloque Vibrations Chocs et Bruits*, France, 2008.

[40] A. Nabhan, M.R. El-Sharkawy, and A. Rashed, "Monitoring of belt-drive defects using the vibration signals and simulation models," *Int. J. Aerosp. Mech. Eng.*, vol. 13, no. 5, pp. 332–339, 2019, doi: 10.5281/zenodo.2702680.

[41] W. Łatas and A. Kot, "Theoretical-experimental determination of CVT power losses due to rubber V-belt vibrations," in A. Puchalski, B.E. Łazarz, F. Chaari, I. Komorska, R. Zimroz (Eds), *Advances in Technical Diagnostics II. ICTD 2022. Applied Condition Monitoring*, vol. 21. Springer, Cham., 2023, doi: 10.1007/978-3-031-31719-4_4.

[42] L. Kong and R.G. Parker, "Approximate eigensolutions of axially moving beams with small flexural stiffness," *J. Sound Vib.*, vol. 276, pp. 459–469, 2004, doi: 10.1016/j.jsv.2003.11.027.

[43] S. Garus *et al.*, "Mechanical vibrations: recent trends and engineering applications," *Bull. Pol. Acad. Sci. Tech Sci.*, vol. 70, no. 1, pp. e140351, 2022, doi: 10.24425/bpasts.2022.140351.